MATEC Web of Conferences **14**, 01002 (2014)
DOI: 10.1051/matecconf/20141401002

Compositional effect on TCP phase formation in Ru-containing Ni-based single crystal superalloys

Qianying Shi[1], Jiajie Huo[2], Lamei Cao[3], Jie Li[2,4], Xianfei Ding[2], Yunrong Zheng[2], and Qiang Feng[1,2,a]

[1] State Key Laboratory for Advanced Metals and Materials, University of Science and Technology Beijing, Beijing 100083, China
[2] National Center for Materials Service Safety, University of Science and Technology Beijing, Beijing 100083, China
[3] Science and Technology on Advanced High Temperature Structural Materials Laboratory, Beijing Institute of Aeronautical Materials, Beijing 100095, China
[4] China Iron and Steel Research Institute Group, Beijing 100081, China

Abstract. Microstructural instability involving the formation of topologically close-packed (TCP) phases is restricted during the alloy development of Ni-based single crystal superalloys. In this study, the effects of alloying elements including Co, Cr, Mo and Ru on the formation of different TCP phases were investigated in a series of single crystal superalloys. Experimental results showed that more additions of Cr and Mo promoted the TCP phase formation, while Co and Ru played a positive role in improving microstructural stability. It is indicated that σ, P and R phases existed with various morphology and compositions in different experimental alloys during thermal exposure at 1100 °C. The content of Co, Cr and Mo in those alloys affected the types of TCP phases significantly, while Ru additions showed a negligible effect. R phase was prone to form in alloys containing high level of Co addition. Meanwhile, the ratio of Cr and Mo content had strong influence on the formation of σ and P phases in alloys containing low level of Co addition. The effects of alloying additions on the elemental partitioning ratios between γ and γ' phases contributed to their corresponding influence on TCP phase formation.

1. Introduction

Ni-based single crystal superalloys with superior mechanical properties at high temperature are widely used for turbine blades in aircraft engines. Micro-structural instability, especially the precipitation of topologically close packed (TCP) phases, should be avoided during alloy development [1]. Many studies indicate that TCP phases, such as σ, μ, P and R phases, are detrimental to mechanical properties, since their hard and brittle nature causes damage accumulation or cracking and their formation depletes the strengthening elements of the γ matrix [2,3].

The precipitation behavior (morphology, composition and kinetics) of different types of TCP phases is influenced by different alloying additions in commercial Ni-based superalloys, which usually contain a combination of five to ten other elements up to 40 wt.% besides Ni [4]. Refractory alloying elements with large differences in electronic structure and atomic radii compared to Ni, such as Mo, W and especially Re, are added for significant solid solution strengthening of the γ matrix in superalloys [4]. Moreover, as one of indispensable alloying elements, Cr is beneficial to hot corrosion and oxidation resistance and also an effective solid solution strengthening element [5]. However, the excessive additions of above mentioned elements were reported to promote the TCP phase formation in Ni-based superalloys [4–6]. As an effective suppressor of TCP phases, Ru was added into the fourth generation single crystal superalloys to improve the microstructural stability and creep properties [7–9]. However, the mechanism is not quite clear yet, and more Ru additions increase the cost of new generation single crystal superalloys. Furthermore, Co additions were found to prevent the formation of TCP phases in some superalloys [8,10–12], although there has been still controversy associated with the effect of Co additions on microstructural stability [13,14].

Alloying effects on microstructural stability, creep capability, environmental resistance and economic cost should be balanced for further alloy development. Although the excessive additons of Cr and Mo could induce a negative effect on microstructural stability, their additions benefit the improvement of creep properties [15,16]. Therefore, it is worthy to evaluate the effects of Cr and Mo additions and maximize their capacity to increase the creep resistance. This will provide the possibility to decrease the level of Re additions, which increases the density and cost of advanced single crystal superalloys and limits their practical application. Since Co was considered to be a potential microstructural stabilizer in previous studies [8,17,18], the role of Co additions in advanced single crystal superalloys should be assessed to investigate whether it is applicable to add more Co as a substitute for a part of expensive Ru to achieve acceptable alloy stability.

[a] Corresponding author: qfeng@skl.ustb.edu.cn

Table 1. Measured chemical compositions (wt.%/at.%) and $\overline{N_v}$ values of experimental single crystal superalloys.

Alloy	Ni	Al	Co	Cr	Mo	Re	Ru	Ta	W	Hf	$\overline{N_v}$
SC1111	Bal.	6.0/14.0	**7.1/7.6**	**3.6/4.4**	**1.0/0.7**	4.4/1.5	**2.6/1.6**	7.9/2.7	5.4/1.9	0.1/0.04	1.95
SC2111	Bal.	6.1/14.1	**15.0/15.9**	**3.5/4.2**	**1.0/0.7**	4.2/1.4	**2.7/1.7**	8.1/2.8	5.5/1.9	0.1/0.04	2.28
SC1211	Bal.	6.0/13.7	**6.9/7.2**	**6.5/7.7**	**1.0/0.6**	4.0/1.3	**2.6/1.6**	7.9/2.7	5.4/1.8	0.1/0.03	2.30
SC1121	Bal.	6.0/13.9	**6.9/7.4**	**3.5/4.2**	**2.4/1.6**	4.1/1.4	**2.7/1.7**	8.0/2.8	5.5/1.9	0.1/0.04	2.03
SC1112	Bal.	6.0/14.1	**6.9/7.4**	**3.5/4.3**	**1.0/0.7**	4.0/1.4	**4.0/2.5**	8.0/2.8	5.4/1.9	0.1/0.04	1.98
SC2221	Bal.	6.0/13.8	**14.4/15.3**	**6.2/7.4**	**2.2/1.4**	4.0/1.3	**2.6/1.6**	8.0/2.7	5.3/1.8	0.1/0.03	2.66
SC2212	Bal.	6.0/13.9	**14.4/15.2**	**6.1/7.3**	**1.0/0.6**	3.9/1.3	**3.7/2.3**	7.9/2.7	5.3/1.8	0.1/0.03	2.60
SC2122	Bal.	6.1/14.2	**14.5/15.5**	**3.5/4.2**	**2.4/1.5**	4.0/1.3	**3.9/2.4**	8.0/2.8	5.4/1.9	0.1/0.04	2.44
SC1222	Bal.	6.0/13.7	**6.7/7.1**	**5.7/7.0**	**2.1/1.4**	3.9/1.3	**3.6/2.2**	7.8/2.7	5.3/1.8	0.1/0.04	2.32

Consequently, on the basis of balancing the individual elemental effects, a series of single crystal superalloys containing different levels of Co, Cr, Mo and Ru additions were designed in this study. An understanding of the individual and synergetic effects of four alloying elements on the formation of TCP phases was acquired through the current work. The information about TCP phase formation in Ru-containing superalloys is helpful to design alloys with better microstructural stability and complement the thermodynamic modelling database.

2. Experimental

The measured chemical compositions of experimental alloys are listed in Table 1. Four elements (Co, Cr, Mo and Ru) were assigned in two levels of contents: low and high (Co: 7.0 wt.% and 15.0 wt.%; Cr: 3.5 wt.% and 6.0 wt.%; Mo: 1.0 wt.% and 2.5 wt.%; Ru: 2.5 wt.% and 4.0 wt.%). These alloys were named as SC plus four numbers, which in turn represented the level of Co, Cr, Mo and Ru additions ("1" and "2" denoting the low and high level of individual elements, respectively). It should be noted that the compositional feature of eight alloys SC2111 ∼ SC1222 is in accordance with the factorial design and then it is applicable to employ associated analysis methods.

These experimental alloys were directionally solidified as single crystal bars with the growth orientation ⟨001⟩ (15 mm in diameter and 150 mm in length) at the Beijing Institute of Aeronautical Materials. The cast experimental alloys were solution heat treated at high temperature in the range of 1300 °C ∼ 1335 °C for 8 ∼ 16 h, and then aged at 1150 °C for 4 h and at 870 °C for 24 h. Following such standard heat treatments, thermal exposure at 1100 °C for different times was performed in order to investigate the alloying effect on the TCP phase formation in these Ru-containing Ni-based single crystal superalloys.

The cross-sectional microstructures perpendicular to the growth orientation of single crystal bars were prepared by the standard metallographic procedure. The TCP precipitates in alloys exposed at 1100 °C for 500 h were separated through the electrolytic phase extraction method in a solution of 9:1 Methanol:HCl + 1 wt.% tartaric acid with a current density of 0.04 A/cm^2, using a stainless steel sheet as a cathode. Microstructural examination was performed using a ZEISS SUPRA 55 field-emission scanning electron microscope (FE-SEM) with an equipped energy-dispersive spectroscope (EDS). Five images taken in the SEM-BSE mode were used for determining the volume fraction of TCP precipitates in each sample through counting the area ratio of TCP phases by using ImagePro Plus software. In order to identify TCP phases, X-ray diffraction (XRD) patterns were obtained from the electrolytic phase extracted residues by Rigaku D/max-RB12 diffractometer with Cu Kα radiation. TEM analyses of the TCP extraction were also carried out to confirm the type of TCP phases in each alloy through selected area electron diffraction patterns using a Tecnai F30 transmission electron microscope.

Electrolytic phase extraction procedure was employed on the alloys after the standard heat treatments to separate the γ' phase. The compositions of γ and γ' phases were obtained through chemical analyses on the residual liquor and residue, respectively. The partitioning ratios of alloying elements between γ and γ' phase, k_i, were calculated through the equation $k_i = c^i_\gamma / c^i_{\gamma'}$, k_i greater or less than unity means that the element i partitions to γ or γ' phase.

Table 2. Volume fraction of TCP precipitates in dendrite cores of experimental alloys after thermal exposure at 1100 °C for different times (%).

Alloy	10h	50h	200h	500h
SC1111	-	-	*	*
SC2111	-	-	*	*
SC1211	6.12 ± 0.42	10.86 ± 0.32	11.23 ± 1.06	11.87 ± 1.014
SC1121	1.20 ± 0.25	5.29 ± 0.66	5.26 ± 0.22	5.65 ± 1.094
SC1112	-	-	-	*
SC2221	0.65 ± 0.31	4.23 ± 1.51	5.39 ± 0.54	5.78 ± 0.75
SC2212	*	*	0.44 ± 0.06	1.19 ± 0.38
SC2122	*	*	0.54 ± 0.16	1.26 ± 0.47
SC1222	8.84 ± 0.87	8.68 ± 0.41	11.53 ± 0.54	10.17 ± 0.79

–, No TCP precipitates; *, Trace of TCP precipitates.

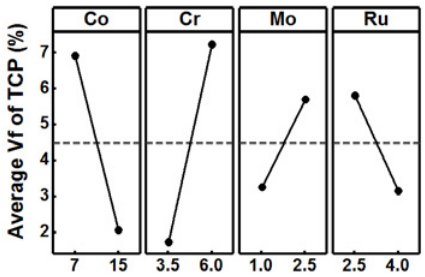

Figure 1. Main effect plots generated by using the volume fractions of TCP precipitates in dendrite cores of alloys SC2111 ∼ SC1222 after thermal exposure at 1100 °C for 500 h.

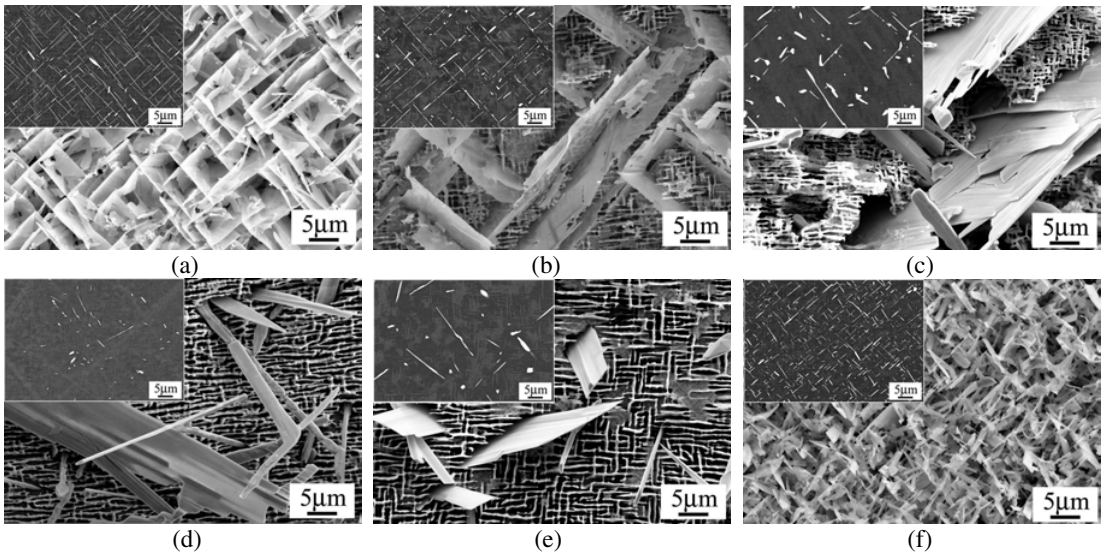

Figure 2. Two-dimensional and three-dimensional morphology of TCP precipitates in experimental alloys after thermal exposure at 1100 °C for 500 h. (a) Alloy SC1211; (b) Alloy SC1121; (c) Alloy SC2221; (d) Alloy SC2212; (e) Alloy SC2122; (f) Alloy SC1222.

3. Results

3.1. The formation of TCP phases

Table 2 shows the volume fraction of TCP precipitates in dendrite cores of experimental alloys after thermal exposure at 1100 °C for time in the range of 10 h to 500 h. It is indicated that these experimental alloys have different tendencies to form TCP phases due to different levels of Co, Cr, Mo and Ru additions. Compared with alloy SC1111, the fact regarding the volume fractions of TCP precipitates in alloys SC1211 and SC1121 indicates that high Cr and Mo contents strongly promoted the TCP phase formation. The further statistical analyses were carried out by using MINITAB software, which generated the plots of main effects to assess the influence of individual elements within alloys SC2111 ∼ SC1222. Figure 1 demonstrates the main effects of four elements generated by using the volume fractions of TCP precipitates in dendrite cores of these eight alloys after thermal exposure at 1100 °C for 500 h. The negative effect of Cr and Mo additions on microstructural stability was again confirmed. In addition, it is indicated that high level of Co and Ru additions decreased the formation of TCP precipitates.

The two-dimensional and three-dimensional morphologies of TCP precipitates in six experimental alloys after thermal exposure at 1100 °C for 500 h are shown in Fig. 2. For alloys SC1211, SC1121 and SC1222, most of TCP precipitates exhibited a needle-like shape in two-dimension, as exhibited in those inserted images at the upper left of Figs. 2a, 2b and 2f. Furthermore, TCP precipitates in alloys SC1211 and SC1222 (Figs. 2a and 2f) appeared to be smooth sheets in three-dimension, which were taken from the phase extracted residues in the matrix. But TCP precipitates in alloy SC1121 showed the sheet morphology with the basket weave in three-dimension (Fig. 2b). As shown in Figs. 2c, 2d and 2e, TCP precipitates in three alloys SC2221, SC2212 and SC2122 primarily appeared to be broadsword-like, and some of them were shown to be short rod-like and needle-like. XRD analyses of the extracted residues in alloys after thermal exposure at 1100 °C for 500 h identified TCP precipitates with different morphologies as different types of TCP phases. Strong peaks of the matrix were observed in all spectra of Figs. 3a–c, suggesting that the extracted TCP precipitates were contaminated by a varying amount of the matrix during the electrolytic phase extraction procedure. A number of peak locations of σ phase (Fig. 3a) showed the considerable correspondence with the TCP precipitates in alloys SC1211 and SC1222. P phase was found to be the best-fitting TCP phase in alloy SC1121 (Fig. 3b), while R phase matched to the majority of diffraction peak locations obtained from the samples of alloys SC2221, SC2212 and SC2122 (Fig. 3c). Figure 4 shows the selected area electron diffraction patterns of σ, P and R phases obtained on the extracted phase residues of alloys SC1211, SC1121 and SC2212. These TEM analyses confirmed the different TCP phases existing in these experimental alloys.

Figure 5 presents the compositional features of different TCP phases, which were obtained through SEM-EDS analyses on the extracted residues of TCP phases in these experimental alloys after thermal exposure at 1100 °C for 500 h. Figures 5a and 5b show that TCP precipitates (mainly σ phase) in alloys SC1211 and SC1222 as well as TCP precipitates (mainly P phase) in alloy SC1121 contained lower Co concentration, while the Co content of the TCP precipitates (mainly R phase) in alloys SC2221, SC2212 and SC2122 was higher (Fig. 5c). The contents of Cr and Mo were approximate in P phase (Fig. 5b), but the ratio of Cr and Mo concentrations was relatively higher in σ phase (Fig. 5a). The slight difference in the Ru content of TCP phases in six experimental alloys was observed in Figs. 5a–c. In addition, Re concentration of σ phase in alloys SC1211 and SC1222 (Fig. 5a) was observed to be higher than in other TCP phases (Figs. 5b and 5c). In fact, the overall compositions of

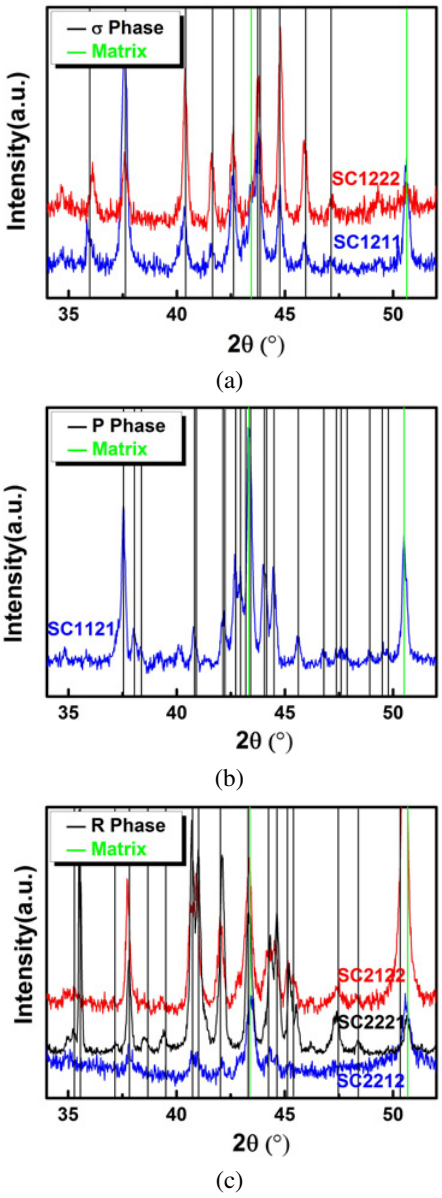

Figure 3. X-ray diffraction patterns of the extracted TCP phases in experimental alloys after thermal exposure at 1100 °C for 500 h. (a) Alloys SC1211 and SC1222; (b) Alloy SC1121; (c) Alloys SC2221, SC2212 and SC2122.

experimental alloys with different levels of Co, Cr, Mo and Ru additions influenced the compositional features of those TCP phases in each alloy. Therefore, it is suggested that the content of Co, Cr and Mo affected the types of TCP phases significantly, while Ru addition showed a negligible effect. R phase was prone to form in alloys containing high level of Co addition (Co concentration in alloys SC2221, SC2212 and SC2122 was at the high level, ~ 15.0 wt.%). Meanwhile, the ratio of Cr and Mo contents (Cr/Mo) had strong influence on the formation of σ and P phases in alloys containing low level of Co addition (Co concentration in alloys SC1211, SC1222 and SC1121 was at the low level, ~ 7.0 wt.%). The Cr/Mo ratios in atomic percent in alloys SC1211 and SC1222 with σ phase

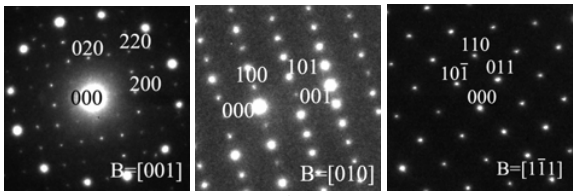

Figure 4. Selected area electronic diffraction patterns of the TCP extraction in the experimental alloys after thermal exposure at 1100 °C for 500 h. (a) σ phase in alloy SC1211; (b) P phase in alloy SC1121; (c) R phase in alloy SC2212.

formation were 12.23 and 4.93, higher than that in alloy SC1121 (2.68) with P phase formation.

3.2. Elemental partitioning ratios between γ and γ' phases

Similar to the elemental partitioning behavior in the majority of Ni-based single crystal superalloys, chemical analyses of γ and γ' phases showed that Al and Ta partitioned into the γ' phase, while Cr, Mo, Re and Ru enriched the γ phase. Additionally, it should be mentioned that the partitioning ratio of W between γ and γ' phases was slightly less than or near to unity in these experimental alloys, which could be attributed to the presence of Re and Ru. Additions of Co, Cr, Mo and Ru influenced the partitioning behaviors of themselves and other alloying elements. Figure 6 exhibits the main effects of these four elements on the partitioning ratios of TCP-forming elements (Cr, Mo, Re and W). It is indicated that more Co and Ru additions decreased the partitioning ratios of Cr, Mo, Re and W to different degrees, while increasing Cr and Mo contents induced the opposite effect.

4. Discussion

The average electron vacancy concentration ($\overline{N_v}$) assigned by considering the electron vacancy number of each element is usually used to predict the formation of TCP phases, since TCP phases are considered as electron compounds [19,20]. Alloys are considered to be TCP-prone if their $\overline{N_v}$ values are above an empirically determined value ($\overline{N_{vc}}$), which varies much in different Ni-based superalloy systems. $\overline{N_v}$ values of these investigated single crystal superalloys in this study were calculated according to the AS5491C standard [21] (as listed in Table 1). Experimental results (Tables 1 and 2) indicated that the alloys with the $\overline{N_v}$ value higher than 2.0 had stronger tendency to form TCP phases during the thermal exposure process. However, the volume fraction of TCP precipitates in alloy SC2111 with the $\overline{N_v}$ value 2.28 was nearly zero even after thermal exposure at 1100 °C for 500 h. Based on the overall composition of alloy SC2111 and the contribution of individual alloying element to the $\overline{N_v}$ value, it is considered that high level of Co additions caused the relatively higher $\overline{N_v}$ value in alloy SC2111. In general, decreasing the level of Co additions in Ni-based superalloys should have a beneficial effect on microstructural stability, since the electron vacancy

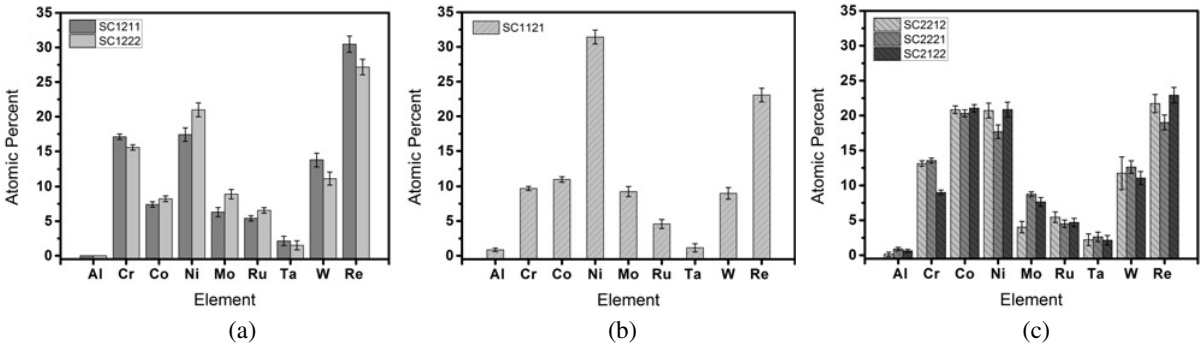

Figure 5. Compositions of TCP precipitates obtained through SEM-EDS analyses on the extracted residues in experimental alloys after thermal exposure at 1100 °C for 500 h. (a) Alloys SC1211 and SC1222; (b) Alloy SC1121; (c) Alloys SC SC2221, SC2212 and SC2122.

number of Co (1.61) is higher than that of Ni (0.66) [13]. Bürgel's study on directionally solidified superalloys showed that Co-free alloy had comparatively more stable microstructure with respect to TCP phase formation than the similar alloy containing 4 wt.% Co [13]. Erickson claimed that lower Co concentrations in a third generation single crystal superalloy CMSX-10 led to the attainment of acceptable alloy stability [14]. However, Co additions were found to prevent the formation of σ phase and μ phase in superalloy MAR-M421 [10] and single crystal superalloy MAR-M247 [11], respectively. Moreover, Walston et al. suggested that high levels of Co additions could induce the reverse partitioning of alloying elements and then improve the resistance to TCP phase formation in a fourth generation single crystal superalloy [8]. Rae's study suggested that Co suppressed the nucleation of the σ phase by altering the γ lattice parameter, which was attributed to the redistribution of elements between γ and γ' phases [6]. Wang's work on a series of single crystal superalloys also demonstrated that TCP phase formation was suppressed by promoting the diffusion process due to more Co additions [12]. In the current study, higher Co addition was showed to be beneficial for the suppression of TCP phase formation, which was attributed to its influence on the elemental partitioning behavior of the TCP-forming elements such as Re, Cr, Mo and W (Fig. 6).

Since the thermodynamic driving force for TCP phases formation results from the solute supersaturation of γ matrix, the elemental partitioning between γ and γ' phases, especially refractory alloying elements such as Re, Mo and W as well as Cr, has strong influence on the formation of TCP phases. It was early reported that Ru additions induced the reverse partitioning behavior of alloying elements between the γ and γ' phases and then suppressed the formation of TCP phases [7]. However, later studies provided contradictory results about the effect of Ru additions on the elemental partitioning behavior [8, 15, 22, 23]. In the current study, increasing Ru addition from $\sim$ 2.5 wt.% to $\sim$ 4.0 wt.% decreased the partitioning ratio of those TCP-forming elements to different degrees (Fig. 6). And more Co additions play the similar role with Ru. This contributed to their suppressive effect on the TCP phase formation. However, increasing Cr and Mo contents increased the partitioning ratios of the TCP-forming elements (Fig. 6). In addition, Cr and Mo were considered as the TCP-forming elements. Accordingly, the

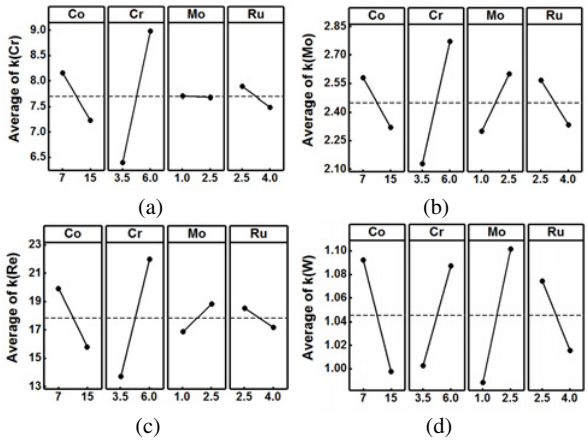

Figure 6. Main effect plots generated by using the elemental partitioning ratios between γ and γ' phases of alloys SC2111 ~SC1222 after the standard heat treatment. (a) k_{Cr}; (b) k_{Mo}; (c) k_{Re}; (d) k_W.

TCP phase formation was promoted by more Cr and Mo additions.

There are limited reports about the effect of alloying additions on the type of TCP phases. Hobb's work suggested that Ru additions affected the compositions of TCP and γ phases as well as their lattice parameters, but no change was observed in the type of TCP phases and the crystallographic orientation relationships between TCP precipitates and matrix [24]. Rae's study reported that increasing the ratio between Mo and W contents stabilized P phase and increasing Cr and Re additions stabilized σ phase [6]. Karunaratne et al claimed that Cr/Mo ratio was a good way for distinguishing between various TCP phases, but the calculated values were not in complete agreement with their experimental results [25]. In the current study, the Re concentration in the σ phase was higher than those of P and R phases, while Ru concentration was similar in three TCP phases (Fig. 5). The content of Co, Cr and Mo in experimental alloys affected the type of TCP phases significantly. R phase was prone to form in alloys containing high level of Co addition. σ and P phases were found in alloys containing low level of Co addition. Meanwhile, the ratio of Cr and Mo contents had strong influence on the formation of σ and P phases. The σ phase

existed in alloys with higher Cr/Mo ratio in comparison with the formation of P phase.

5. Conclusions

Microstructural instability involving the formation of TCP phases was investigated in a series of single crystal superalloys containing different levels of Co, Cr, Mo and Ru additions in this study. The following conclusions can be drawn:

(1) TCP phases existed with various morphologies and compositions in different experimental alloys during the thermal exposure at 1100 °C. More additions of Cr and Mo promoted the TCP phase formation, while Co and Ru had a positive effect on microstructural stability.

(2) Co and Ru additions decreased the partitioning ratios of Re, Cr, Mo and W to different degrees, while increasing Cr and Mo contents induced the opposite effect. Effects of these four alloying additions on the elemental partitioning behavior between γ and γ' phases contributed to their corresponding influence on TCP phase formation.

(3) The contents of Co, Cr and Mo in these alloys affected the types of TCP phases significantly, while Ru additions showed a negligible effect. Alloys containing high level of Co addition had a tendency to R phase formation after thermal exposure at 1100 °C. Meanwhile, the formation of σ and P phases were prone to form in alloys containing low level of Co addition. σ phase existed in alloys with higher Cr/Mo ratio in comparison with the formation of P phase.

The financial supports provided by National Natural Science Foundation of China (Grant No. 51271015), National Basic Research Program of China (Grant No. 2010CB631201) and National High Technology Research and Development Program of China (Grant No. 2012AA03A513 and 2012AA03A511) are gratefully acknowledged.

References

[1] R.C. Reed, *The superalloys: Fundamentals and applications*, (Cambridge University Press, Cambridge, 2006)
[2] A.C. Yeh, A. Sato, T. Kobayashi, H. Harada, Mater. Sci. Eng. A, **490,** 445 (2008)
[3] M. Pessah, P. Caron, T. Khan, *Superalloys 1992*, TMS, 567 (1992)
[4] T.M. Pollock, S. Tin, Journal of Propulsion and Power, **22**, 361 (2006)
[5] J.Y. Chen, Q. Feng, L.M. Cao, Z.Q. Sun, Mater. Sci. Eng. A, **528**, 3791 (2011)
[6] C.M.F. Rae, R.C. Reed, Acta Mater., **49**, 4113 (2001)
[7] K.S. O'Hara, W.S. Walston, E.W. Ross, R. Darolia, US Patent: *5482789* (1996)
[8] S. Walston, A. Cetel, R. MacKay, K. O'Hara, D. Duhl, R. Dreshfield, *Superalloys 2004*, TMS, 15 (2004)
[9] L.J. Carroll, Q. Feng, T.M. Pollock, Metall. Mater. Trans. A, **39**, 1290 (2008)
[10] C.H. Lund, M.J. Woulds, J. Hockin, *Superalloys 1968*, TMS, 25 (1968)
[11] T.E. Strangman, G.S. Hoppin III, C.M. Phipps, K. Harris, R.E. Schwer, *Superalloys 1980*, TMS, 215 (1980)
[12] W.Z. Wang, T. Jin, J.L. Liu, X.F. Sun, H.R. Guan, Z.Q. Hu, Mater. Sci. Eng. A, **479,** 148 (2008)
[13] R. Bürgel, J. Grossmann, O. Lusebrink, H. Mughrabi, F. Pyczak, R.F. Singer, A. Volek, *Superalloys 2004*, TMS, 25 (2004)
[14] G.L. Erickson, *Superalloys 1996*, TMS, 35 (1996)
[15] L.J. Carroll, Q. Feng, J.F. Mansfield, T.M. Pollock, Metall. Mater. Trans. A, **37**, 2927 (2006)
[16] J. Zhang, T. Murakumo, Y. Koizumi, T. Kobayashi, H. Harada, Metall. Mater. Trans. A, **35**, 1911 (2004)
[17] R.A. MacKay, T.P. Gabb, A. Garg, R.B. Rogers, M.V. Nathal, NASA Report: *20120017919* (2012)
[18] Q. Shi, X. Ding, M. Wang, Y. Zheng, J. He, S. Tin, Q. Feng, Metall. Mater. Trans. A, **45**, 1833 (2014)
[19] N. Yukawa, H. Adachi, *Superalloys 1984*, TMS, 523 (1984)
[20] J. Zhang, Z. Hu, Y. Ata, M. Morinaga, N. Yukawa, Metall. Mater. Trans. A, **24**, 2443 (1993)
[21] SAE International Standard, AS5491C: Calculation of Electron Vacancy Number in Superalloys (2007)
[22] R.C. Reed, A.C. Yeh, S. Tin, S.S. Babu, M.K. Miller, Scripta Mater., **51**, 327 (2004)
[23] T. Yokokawa, M. Osawa, K. Nishida, T. Kobayashi, Y. Koizumi, H. Harada, Scripta Mater., **49**, 1041 (2003)
[24] R.A. Hobbs, L. Zhang, C.M.F. Rae, S. Tin, Metall. Mater. Trans. A, **39**, 1014 (2008)
[25] M. Karunaratne, C. Rae, R. Reed, Metall. Mater. Trans. A, **32**, 2409 (2001)